Drug Design, Development and Therapy

Dovepress
open access to scientific and medical research

Open Access Full Text Article

ORIGINAL RESEARCH

Increased therapeutic efficacy of a newly synthesized tyrosinase inhibitor by solid lipid nanoparticles in the topical treatment of hyperpigmentation

This article was published in the following Dove Press journal:
Drug Design, Development and Therapy
2 December 2016
Number of times this article has been viewed

Md Al-Amin
Jiafu Cao
Muhammad Naeem
Hasanul Banna
Min-Soo Kim
Yunjin Jung
Hae Young Chung
Hyung Ryong Moon
Jin-Wook Yoo

College of Pharmacy, Pusan National University, Busan, South Korea

Abstract: Hyperpigmentation caused by melanin overproduction is a major skin disorder in humans. Inhibition of tyrosinase, a key regulator of melanin production, has been used as an effective strategy to treat hyperpigmentation. In this study, we investigated the use of solid lipid nanoparticles (SLNs) as a highly effective and nontoxic means to deliver a newly synthesized potent tyrosinase inhibitor, MHY498, and to target melanocytes through the skin. MHY498-loaded SLNs (MHY-SLNs) were prepared by an oil-in-water emulsion solvent-evaporation method, and their morphological and physicochemical properties were characterized. MHY-SLNs showed a prolonged drug-release profile and higher skin permeation than that of MHY solution. In an in vivo evaluation of antimelanogenic activity, MHY-SLNs showed a prominent inhibitory effect against ultraviolet B-induced melanogenesis, resulting in no change in the skin color of C57BL/6 mouse, compared with that observed in an MHY solution-treated group and an untreated control group. The antimelanogenic effect of MHY-SLNs was further confirmed through Fontana–Masson staining. Importantly, MHY-SLNs did not induce any toxic effects in the L929 cell line. Overall, these data indicate that MHY-SLNs show promise in the topical treatment of hyperpigmentation.

Keywords: melanogenesis, hyperpigmentation, MHY498, solid lipid nanoparticles, skin delivery

Introduction

Melanin is a determinant of skin color and produced by the melanogenesis pathway[1] in melanocytes located in the basal layer of the epidermis. It plays an important role in protecting skin against ultraviolet (UV)-induced damage;[2,3] however, melanin overproduction causes hyperpigmentation including freckles, melisma, and lentigines, which is the third most common dermatological disorder related to serious esthetic problems owing to its visible nature.[4–6] Various causative factors, such as UV radiation, alpha-melanocyte-stimulating hormone (α-MSH), cyclic AMP-elevating agents (such as forskolin),[7,8] and melanin-synthesizing enzymes (such as tyrosinase, tyrosinase-related protein 1, and dopachrome tautomerase),[9] have been studied to regulate melanin production and skin accumulation. Among them, inhibition of tyrosinase has emerged as an effective strategy to treat hyperpigmentation because tyrosinase controls the rate-limiting steps of melanogenesis where tyrosine is converted to dopaquinone, which subsequently produces eumelanin and pheomelanin.[10,11]

Correspondence: Jin-Wook Yoo
College of Pharmacy, Pusan National University, 2 Busandaehak-ro, 63 Beon-gil, Geumjeong-gu, Busan 609-735, South Korea
Tel +82 51 510 2807
Fax +82 51 513 6754
Email jinwook@pusan.ac.kr

submit your manuscript | www.dovepress.com
Dovepress
http://dx.doi.org/10.2147/DDDT.S123759

Conventional tyrosinase inhibitors such as kojic acid and hydroquinone have been used as skin-whitening agents in sunscreen and cosmetic formulations.[12] Their clinical uses, however, have been limited because of poor in vivo efficacy, poor skin permeation, and/or low formulation stability.[13,14] This has led to the development of new tyrosinase inhibitors. Recently, a novel tyrosinase inhibitor – (*Z*)-5-(2,4-dihydroxy benzylidene)thiazolidine-2,4-dione (MHY498) – was synthesized based on the fact that compounds containing imidazole and 2,4-dihydroxy phenyl moiety inhibit tyrosinase activity more potently than other derivatives.[15,16] MHY498 (mean IC_{50} [the half maximal inhibitory concentration]=3.55 μM) is 6.4-fold more potent than kojic acid (mean IC_{50}=22.79 μM), a positive standard and the most intensively studied tyrosinase inhibitor.[15] Moreover, MHY498 was not cytotoxic to B16F10 melanoma cells at concentrations of up to 32 μM, while it inhibited tyrosinase in a dose-dependent manner. Kojic acid was cytotoxic at the same concentration.[15] Thus, MHY498 appears to be a promising tyrosinase inhibitor for treating hyperpigmentation.

Despite its potency, MHY498's delivery through the skin is a major hurdle owing to the stratum corneum, which functions as a primary skin barrier.[17] The low delivery efficiency would necessitate frequent administration or the use of permeation enhancers, which compromise patients' compliance or may cause skin toxicity. Moreover, direct contact of tyrosinase inhibitors with the stratum corneum may cause skin carcinogenesis.[18] Thus, a delivery system that ensures efficient penetration through the stratum corneum to melanocytes with safe MHY498 encapsulation (to avoid direct skin contact) is needed.

Solid lipid nanoparticles (SLNs) have long been used as a topical drug-delivery system because they eliminate the traditional disadvantages encountered during drug delivery through the skin.[19,20] SLNs have unique features over other nanoparticle systems, which make SLNs a potential useful skin delivery system. Lipids used in SLNs are biocompatible and recognized as safe excipients that are devoid of acute and chronic dermal toxicity.[21,22] Furthermore, lipids can have a beneficial interaction with the stratum corneum, which is composed of hexagonal corneocytes embedded in a lipid matrix of ceramide, free fatty acids, cholesterol, and triglycerides.[23] When SLNs are applied to the skin, they form an occlusive film that prevents transepidermal water loss and hydrates the stratum corneum.[20,24] Thus, corneocyte packing of the stratum corneum becomes loose, which facilitates drug penetration.

To date, a few studies have been reported regarding the formulation of lipid nanoparticles containing tyrosinase inhibitors.[25–29] However, most were confined to in vitro characterizations, and no extensive in vivo evaluation of hyperpigmentation treatment has been performed. Our main focus in this study was to deliver MHY498 into the basal layer of the epidermis using SLNs as carriers to effectively inhibit melanogenesis. We encapsulated MHY498 in lipid nanoparticles based on Compritol 888 ATO. Formulated SLNs were characterized using different parameters, and their in vivo melanogenesis inhibition efficacies were evaluated in a C57BL/6 mouse model. The toxicity profile of MHY498-loaded SLNs (MHY-SLNs) was evaluated in L929 skin fibroblast cells.

Materials and methods

Materials

(*Z*)-5-(2,4-dihydroxy benzylidene)thiazolidine-2,4-dione (MHY498) was synthesized as previously reported.[13] Glyceryl behenate (Compritol 888 ATO) was generously gifted by Gattefossé (Saint-Priest, France). Phospholipon 90 G (phosphatidylcholine 90%) was a gift from Lipoid GmbH (Ludwigshafen, Germany). Poloxamer 188 (Kolliphor® P 188), phosphotungstic acid, tetrazolium dye 3-(4,5-dimethylthiazol-2-yl)-2,5-diphenyltetrazolium bromide (MTT), and dimethyl sulfoxide (DMSO) were purchased from Sigma-Aldrich (St Louis, MO, USA). Roswell Park Memorial Institute (RPMI) 1640 medium, trypsin, fetal bovine serum, and penicillin–streptomycin were purchased from Hyclone (Logan, UT, USA). The Fontana–Masson Staining Kit was purchased from ScyTek (Logan, UT, USA). All other reagents and solvents were of the highest analytical grade commercially available.

Preparation of MHY-SLNs

MHY-SLNs were prepared by a modified oil-in-water emulsion solvent-evaporation method.[30] Briefly, 10 mg MHY498, 150-mg Compritol 888 ATO, and 100 mg Phospholipon 90 G were dissolved in 10 mL of anhydrous ethanol and heated at 80°C, which constituted the organic phase. The organic phase was slowly injected into 0.5% w/v cold poloxamer solution. The mixture was stirred at 1,000 rpm for 4 h in a fume hood, and the solvent was evaporated. The resultant SLNs were harvested by centrifugation at 15,000 rpm for 1 h. The obtained pellet was reconstituted in water and stored as a suspension. To evaluate crystallinity, MHY-SLNs suspension was freeze-dried at −50°C for 24 h.

Physicochemical characterization of MHY-SLNs by transmission electron microscopy (TEM)

MHY-SLNs morphology was investigated by TEM (H-7600, Hitachi, Japan), using a negative-staining method.[31] Briefly,

1 drop of diluted MHY-SLNs suspension was mounted on a 200-mesh formvar copper grid and dried at room temperature. Then, the sample was negatively stained with 1% (w/v) phosphotungstic acid and viewed by TEM.

Determination of particle size and analysis

Particle sizes and zeta potentials of MHY-SLNs were measured using a Malvern Zetasizer Nano ZS system (Malvern Instruments, Worcestershire, UK). Briefly, 5 µL of each SLN sample was diluted in 2 mL Milli-Q water, and particle sizes and zeta potentials were measured at 25°C.

Drug loading and encapsulation efficiency

The amount of MHY498 in SLNs was determined by UV spectrophotometry with some modifications. Briefly, 200 µL MHY-SLNs suspension was freeze-dried and dissolved in anhydrous ethanol. An ethanolic solution containing MHY498 was shaken overnight using a vortexer. Subsequently, the solution was centrifuged at 12,000 rpm for 20 min. The supernatant was collected and analyzed by UV spectrophotometry at 376 nm. All experiments were performed in triplicate. From these measurements, the total amount of MHY498 in SLNs and weight of SLNs were calculated. Drug loading and the encapsulation efficiency (%) were calculated using the following equations:

$$\text{Drug loading (\%)} = \frac{\text{MHY} - 498 \text{ in SLNs (mg)}}{\text{Total SLNs weight (mg)}} \times 100 \quad (1)$$

$$\text{Encapsulation efficiency (\%)} = \frac{\text{Amount of MHY} - 498 \text{ in SNSs (mg)}}{\text{Amount of MHY} - 498 \text{ initially added (mg)}} \times 100 \quad (2)$$

X-ray diffraction (XRD)

The physical status of MHY498 in SLNs was analyzed by XRD analysis using a Rigaku XRD (MiniFlex, Rigaku, Tokyo, Japan). The X-ray tube was run at 40 kV and 40 mA. Scattering angles were transformed into short spacings using Bragg's equation ($n\lambda=2d\sin\theta$). All powdered samples were scanned in the 2θ range of 5°C–40°C, and the scanning rate was 2θ/min. Samples included MHY498 alone, bulk Compritol 888 ATO, and MHY-SLNs.

Differential scanning calorimetry (DSC)

DSC was performed using a DSC-8000 (Perkin-Elmer, Waltham, MA, USA). A heating rate of 10°C/min was applied in 20°C–220°C temperature range. Analysis was performed under a nitrogen purge of 20 mL/min. Approximately, 10 mg of sample was used for analysis. Samples included MHY498 alone, bulk Compritol 888 ATO, and MHY-SLNs. An empty aluminum sample pan was used as a reference.

In vitro release study

MHY498 in vitro release from SLNs was determined by the dialysis bag-diffusion technique.[32] Dialysis bags with a molecular weight cutoff of 12,000–14,000 (Visking® dialysis tubing, Servia, Greece) were used. Release medium contained 150 mL phosphate-buffered saline (PBS, pH 7.4) with 1% Tween 80. Dialysis membranes were soaked overnight and filled with 3 mL of MHY-SLNs suspension. Dialysis membranes were sealed at both ends and placed into the release medium. Experiments were performed at 37°C, with a stirring speed of 50 rpm. Samples were withdrawn at 0.5, 1, 2, 3, 4, 6, 8, 12, 24, and 48 h. At each sampling point, 1 mL of sample was withdrawn and replaced with fresh medium. The withdrawn sample was analyzed by UV spectrophotometry. The release from each formulation was measured in triplicate.

In vitro skin-permeation study

In vitro skin-permeation studies were performed using a 3-station Franz diffusion cell (PermeGear, Inc., Hellertown, PA, USA). Full-thickness dorsal skin from C57BL/6 mice (male, 7 weeks, 25 g) was used. Animal study protocols were approved by the Animal Care Committee of Pusan National University and were performed, following the guidelines for animal experiments issued by Pusan National University. Briefly, each mouse was euthanized using CO_2 gas. Subsequently, hair from the dorsal portion was carefully removed using an electric trimmer. Application of Veet® Hair Removal Cream (Reckit Benckiser, Inc., Slough, UK) for 5 min facilitated complete hair removal. The skin was collected, and subcutaneous fatty tissues were removed using blunt tweezers with simultaneous washing with PBS. The Franz diffusion cell was connected with a circulatory water jacket to maintain the temperature at 37°C. The receptor compartment was filled with 7 mL PBS (pH 7.4) and 1 mL ethanol. Ethanol was used as a solubilizer to ensure a sufficient sink condition. Mouse skin was mounted on the cell with the stratum corneum side facing outside. The diffusion area of the skin was 0.95 cm^2. The donor compartment was filled with a 300 µg equivalent of MHY-SLNs suspension and covered with paraffin to prevent evaporation. The receptor solution was stirred at constant rpm at predetermined time points (0.5, 1, 2, 3, 4, 6, 12, 24, and 48 h). Next, 2 mL of sample was withdrawn and replaced with the same volume of fresh solution. All samples were filtered through an aqueous

0.22 µm pore size cellulose membrane filter and analyzed by UV spectrophotometry. A similar procedure was performed for MHY solution containing 300 µg of MHY498 at a 2:1 ratio of ethanol:propylene glycol.

Skin-permeation parameters

The cumulative amount (Q_{MHY}) of MHY498 that permeated through mouse skin was plotted against time and determined using the following equation:

$$Q_{MHY} = \frac{Vr\ X\ Ct + \sum_{i=0}^{t-1} Vd\ X\ Ci}{A} \quad (3)$$

Here, Vr and Vd are the volume of the receptor and sample taken at each sampling time, respectively. Ct indicates the MHY498 concentration of the receptor compartment at each sampling time. Ci is the drug concentration of the *i*th sample. *A* is the effective skin surface area (0.95 cm^2). MHY498 flux through the skin, J (µg/cm^2·h), was calculated from the slope of a linear portion of a graph showing the cumulative amount of MHY498 permeating through mouse skin per unit surface area versus time.

In vivo evaluation of MHY-SLNs

To evaluate the depigmentation activity of MHY-SLNs, C57BL/6 mice were used as a model in animal experiments. Five-week-old male C57BL/6 mice were purchased from Samtako Bio (Osan, South Korea). Mice were housed under standard conditions with a 12 h/12 h light/dark cycle and fed standard food and drinking water. The animals were acclimatized for 7 days before initiating experiments. The dorsal side of mouse skin was used for the experiments. Mouse hair was removed using an electric trimmer and Veet Hair Removal Cream.

Mice were randomly divided into 4 groups of 6 animals per group: UV control, MHY solution, blank-SLNs, and MHY-SLNs. Each group was irradiated with UVB radiation at an intensity of 450 mJ/cm^2 using a crosslinker (BEX-800, Ultra-Lum, Claremont, CA, USA) to induce melanogenesis in the mouse dorsal skin. Each group was exposed to UVB radiation for 2 weeks on alternate days. A 2×2 cm^2 area was selected, and a 200 µg/mL equivalent of MHY-SLNs suspension or MHY solution alone was applied to the mouse skin for 14 days in the MHY-SLNs and MHY solution groups, respectively. The UV control group was untreated.

During treatment, skin brightness was measured using a CR-10 spectrophotometer (Konica Minolta Sensing, Sakai, Osaka, Japan), which describes colors using *L**, *a**, and *b** values as described by the Commission Internationale de l'Eclairage color system.[33] Mice were sacrificed after 14 days, and designated skin portions were collected for histological evaluation.

Histological evaluation

Skin biopsy specimens were fixed in 10% formaldehyde solution for 24 h and embedded in a paraffin block according to standard procedures. Sections (5 µm thick) were fixed to glass slides and stained with Fontana–Masson stain to observe melanocytes and melanin. Slides were examined by light microscopy, and images were digitally captured without further processing.

In vitro cytotoxicity study using L929 skin cytotoxicity cells

The mouse fibroblast cell line L929 obtained from the Korean Cell Line Bank (KCLB, Seoul, South Korea) were cultured in RPMI 1640 medium supplemented with 10% (v/v) fetal bovine serum, 100 IU/mL penicillin G sodium, and 100 µg/mL streptomycin sulfate. The cells were grown at 37°C in an incubator supplied with 5% CO_2 and a humidified air atmosphere. Cells were seeded in 96-well plates at 5×10^4 cells per well and incubated for 24 h. The media were then replaced with fresh media containing MHY-SLNs suspension and MHY solution containing different MHY498 concentrations (50, 100, 200, and 400 µg/mL) and incubated for 24 h. A standard MTT solution in sterile PBS was added to each well and incubated for 2 h. Media containing test substances and MTT solution were then removed, and 150 µL of DMSO was added to each well. The absorbance measured at 540 nm was proportional to the concentration of viable cells in each well. Untreated cells were used as a control. The data were expressed as the mean ± standard deviation (SD) of 4 replication (n=4). Cell viability was calculated using the following equation:

$$\text{Cell viability (\%)} = \frac{\text{Absorbance (treated)}}{\text{Absorbance (control)}} \times 100 \quad (4)$$

Statistical analysis

The results are expressed as the mean values (±SD) of 3–6 experiments. All in vivo data analysis was performed using an unpaired Student's *t*-test in GraphPad Prism 5.0 (GraphPad Software, Inc., La Jolla, CA, USA). *P*-values of <0.05 were considered statistically significant.

Results and discussion

MHY-SLNs preparation and characterization

MHY-SLNs were prepared by a modified emulsion solvent-evaporation method.[28] Organic MHY498, Compritol 888 ATO, and Phospholipon 90 G were used as the organic phase, and poloxamer 188 was used as the aqueous phase. When hot organic phase was injected into hot poloxamer 188 solution, the yield of SLNs was very low (~25%). We found that hot poloxamer 188 solubilized MHY498, which might have caused expulsion of MHY498 from the SLN matrix. To avoid MHY498 expulsion, the hot organic phase was injected into a cold poloxamer 188 solution and stirred at 4°C. This modification resulted in a facile formulation of MHY-SLNs with a high yield (88.5%) and sufficient drug (3.4%) loading. The physicochemical characterization of the MHY-SLNs is shown in Table 1.

Size is an important parameter for the occlusive properties of SLNs. In general, SLNs particle size <400 nm possess occlusive properties that promote skin penetration.[24,32] From a size-distribution histogram (Figure 1A), it can be seen that the MHY-SLNs were fabricated with a particle size of <400 nm. The TEM image also confirmed the particle sizes of MHY-SLNs are shown in Figure 1B. The smaller particle sizes observed by TEM (as compared to dynamic light scattering calorimetry [DLS] measurements) can be explained by the fact that DLS measures the hydrodynamic diameter, whereas TEM measures the particle cores only. Zeta potentials provide information regarding the stability of aqueous colloidal dispersions.[34] Particles with high zeta potential values (>|30| mV) have a reduced tendency to aggregate.[35] SLNs are negatively charged on the surface.[36] MHY-SLNs showed a zeta potential value of −29.8 mV, which confirmed that MHY498 loading into an SLNs matrix did not affect particle stability (Table 1).

XRD and DSC are widely used techniques for determining the physical status of SLNs matrixes. XRD and DSC data help identify whether a drug is loaded into the particle matrix. XRD data for MHY498, bulk Compritol 888 ATO, and freeze-dried MHY-SLNs are represented in Figure 1C. Each sample has characteristic crystalline domains that can be identified through XRD by scanning over a wide range of incident angles. The XRD pattern of MHY498 showed several narrow peaks with a maximum peak intensity at 2θ=27.5°C, indicating its crystallinity. Compritol only showed 2 sharp peaks with a maximum at 2θ=21.18°C. In the MHY-SLNs diffractogram, 1 major peak was observed at 2θ=21.29°C, which appeared to overlap with the Compritol diffractogram. It was also noted that the MHY498-specific peaks disappeared in the diffractogram for MHY-SLNs, indicating an amorphous or molecularly dispersed state in the SLN matrix.[37] The degree of crystallinity is related to peak intensity. Sharp peaks indicate a highly crystallized particle state, whereas narrow peaks are indicators of low crystallinity.[38] In MHY-SLNs, the peak intensity was reduced when compared with Compritol, demonstrating a decreased crystallinity of MHY-SLNs. DSC measures the crystallinity of samples based on their corresponding melting enthalpies or melting points. Thermograms of MHY498, bulk Compritol 888 ATO, and freeze-dried MHY-SLNs are represented in Figure 1D. The thermogram of MHY-SLNs did not show a melting peak for crystalline MHY498 at 110°C, meaning that MHY498 adopted an amorphous state in the SLN matrix. In this study, MHY498 and Compritol were dissolved in anhydrous ethanol. Therefore, MHY498 was dispersed in the lipid homogenously. This result is consistent with that of a previous report showing podophyllotoxin in SLNs in an amorphous state.[39] The melting point of Compritol (79°C) was slightly reduced in MHY-SLNs (76°C), suggesting that the β form of SLNs was adopted.[40] This melting point depression might be due to the small particle size (nanometer range), high surface area, and presence of surfactant.[38]

In vitro release study

Simulation-based in vitro release experiments were performed to determine drug-release behavior from the particle matrix. The release pattern observed following in vitro release helps in determining the dose and treatment period in real in vivo settings. As represented in Figure 2, MHY-SLNs showed a biphasic release pattern. Nearly, 70% of MHY498 was released from SLNs matrix within first 6 h, which fits the Higuchi kinetic model (R^2=0.996). This initial fast release of MHY498 might play a key role in enhancing skin penetration, as it increases the concentration gradient to provide higher drug diffusion through the skin.[20] The remainder of

Table 1 Physicochemical characterization of MHY-SLNs

Formulation	Yield (%)	DL (wt %)	EE (%)	Size (nm)	Zeta potential (mV)	PDI
MHY-SLNs	88.5±1.7	3.4±0.4	77.6±4.7	207±39	−29.8±1.2	0.269

Note: Values are presented as the mean ± SD (n=3).
Abbreviations: DL, drug loading; EE, encapsulation efficiency; MHY-SLNs, MHY498-loaded solid lipid nanoparticles; PDI, polydispersity index; SD, standard deviation.

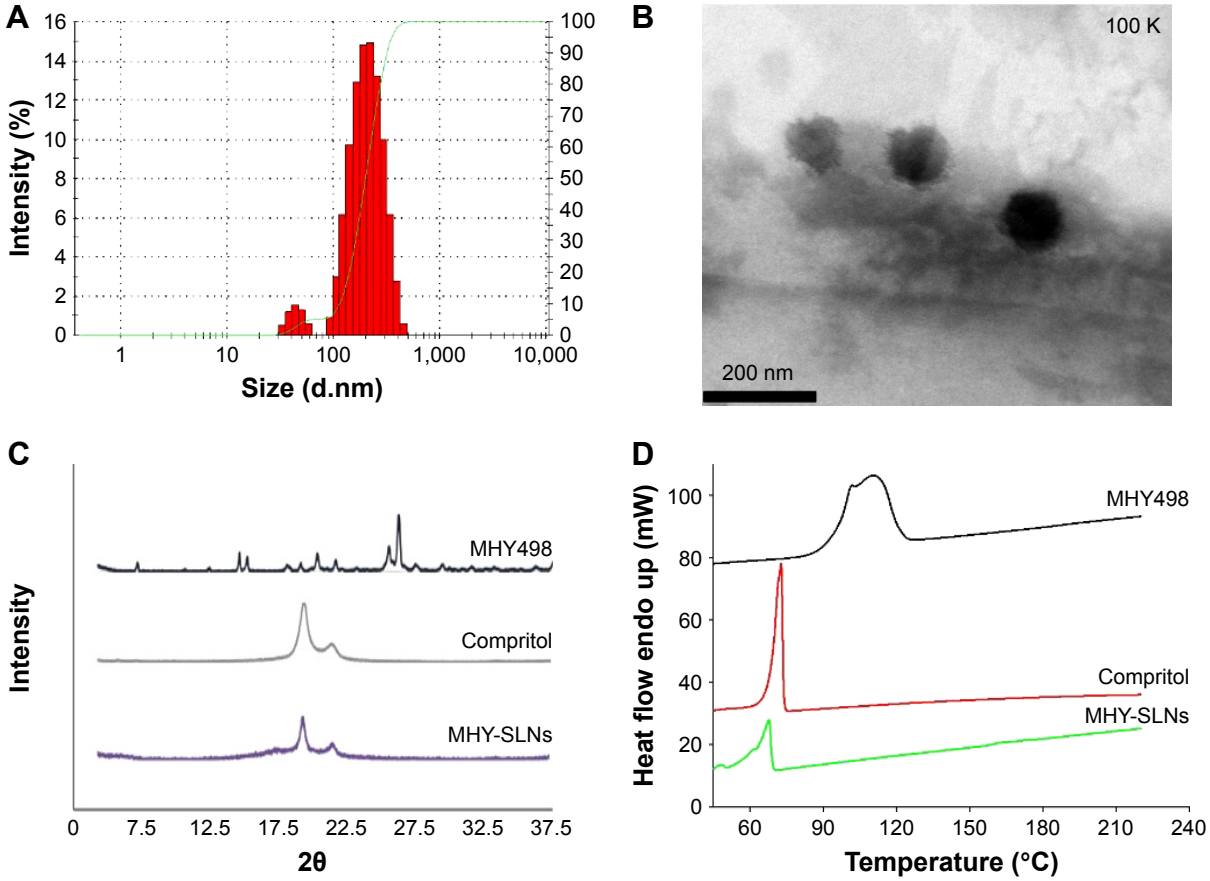

Figure 1 In vitro characterization of MHY-SLNs.
Notes: Transmission electron microscopy images (**A**), particle size distribution (**B**), X-ray diffraction analysis diffractograms (**C**) and differential scanning calorimetry thermograms (**D**) of MHY498, Compritol, and MHY-SLNs.
Abbreviations: MHY-SLNs, MHY498-loaded solid lipid nanoparticles; endo, endothermic.

the MHY498 (>90%) was released over 48 h, confirming the prolonged-release characteristics of MHY-SLNs.[41] The amorphous form of the drug allows slow diffusion leading to prolonged release from SLN matrixes.[42] The XRD and DSC data of MHY-SLNs demonstrated the amorphous state of MHY498 in SLN matrixes (Figure 1). This biphasic release pattern could be important in skin delivery. The initial fast release can facilitate MHY498 skin permeation by providing a sufficient concentration gradient, whereas the sustained release maintains the local concentration, leading to a prolonged antimelanogenesis effect of MHY498.

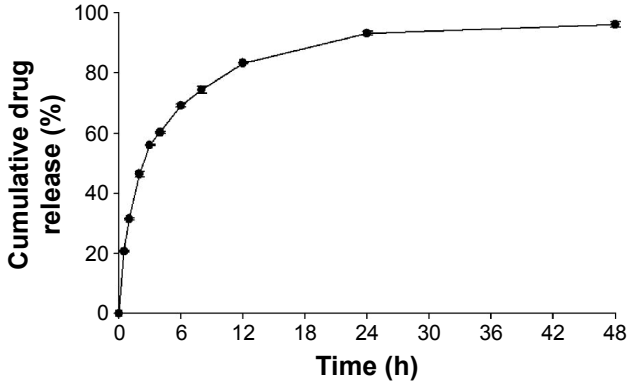

Figure 2 In vitro release profile of MHY498-loaded solid lipid nanoparticles.
Notes: A drug-release study was performed using the dialysis bag-diffusion technique. Results are presented as the mean ± SD (n=3).
Abbreviation: SD, standard deviation.

In vitro skin-permeation study

The skin permeability of MHY-SLNs was evaluated and compared with that of the MHY solution. MHY498 is a poor water-soluble drug. It is poorly soluble in common organic solvents, such as dichloromethane, chloroform, and acetone. Solubility of MHY498 is only prominent in low-molecular weight alcohol, such as methanol, ethanol, propylene glycol, and DMSO. Among them, ethanol and propylene glycol are widely used as emollients, solvents, and penetration enhancers in various topical dosage forms.[43] A 2:1 ratio of ethanol:propylene glycol was used as a solvent for MHY solution. DMSO was excluded from the study considering its smell that may hamper the aesthetic appeal of

cosmetics or topical dosage form. Figure 3 demonstrates the skin-penetration pattern of MHY solution and MHY-SLNs. MHY-SLNs showed higher skin permeation than did the MHY solution. In the case of MHY solution, it took 4 h to initiate skin permeation. A lag time is a common phenomenon in skin-permeation studies. A similar lag time for ethanol and propylene glycol was previously reported.[44] This might be due to the fact that using propylene glycol can cause skin tortuosity by dehydrating the stratum corneum, resulting in a sufficiently increased diffusional length to enable passage through the skin.[45] However, MHY498 skin permeation from the SLN matrix began only after 30 min, which led to higher overall permeation than observed with the MHY solution after 48 h. Flux is another parameter used to evaluate skin permeability by measuring the amount of material crossing the skin per unit area per unit time. The flux at different time intervals (12, 24, and 48 h) was determined, and the results demonstrated that MHY-SLNs showed a 2-fold higher flux than did the MHY solution, in that 2 times more MHY498 from MHY-SLNs permeated through the skin than did MHY from MHY solution (Table 2). The high skin permeability of MHY-SLNs may result from the film-formation ability of SLNs, which is absent in solution formulations. Film formation causes skin hydration by preventing transepidermal water loss. The tightly arranged stratum corneum becomes swollen, corneocyte packing becomes loose, and MHY498 effectively permeates the skin through an intracellular route (Figure 4).

In vivo evaluation of MHY-SLNs

The in vivo efficacy of MHY-SLNs was evaluated based on qualitative and quantitative brightness comparisons.

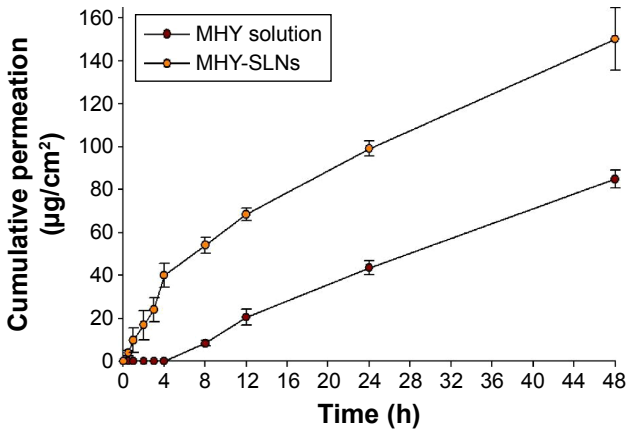

Figure 3 In vitro skin permeation of MHY solution and MHY-SLNs.
Notes: In vitro skin permeability was evaluated using C57BL/6 mouse dorsal skin. Results are presented as the mean ± SD (n=3).
Abbreviations: MHY-SLNs, MHY498-loaded solid lipid nanoparticles; SD, standard deviation.

Table 2 Flux determination of MHY-SLNs and MHY solution at different time intervals

Formulation	Flux (J) (µg/cm²·h)		
	12 h	24 h	48 h
MHY-SLNs	5.7±1.1	4.1±0.4	3.3±0.6
MHY solution	1.7±0.5	1.8±0.3	1.8±0.1

Note: Values are presented as the mean ± SD (n=3).
Abbreviations: MHY-SLNs, MHY498-loaded solid lipid nanoparticles; SD, standard deviation.

C57BL/6 mouse dorsal skin was irradiated with UVB radiation. UVB radiation can penetrate the epidermal layer of the skin. UVB radiation (290–320 nm) increased MSH receptor activity on cutaneous melanocytes, which caused UVB-induced melanogenesis.[46,47] Thus, melanocyte production increased and accumulated in the basal epidermal layer. Such melanocytes were responsible for skin darkening and pigmentation.[48,49] Figure 5A and B represents the qualitative and quantitative skin-brightness comparisons, respectively, among the different groups tested. The *L* value is an indicator of skin brightness, where *L* values of 64–68 denote bright skin and *L* values of 40–45 denote dark skin. Before initiating UV radiation and treatment, the skin tissues were relatively bright with *L* values of 65±2. In the untreated group (UV control), UV radiation administered on alternate days over a 14-day period made the skin dark, and *L* value drops down to 40 (Figure 5B). In the MHY solution group, a gradual decrease of skin brightness was observed, but the skin remained brighter than the untreated group. In contrast, skin brightness was nearly unchanged after 14 days in the MHY-SLNs group. As mentioned above, MHY498 from an SLN matrix permeates the skin easily due to its occlusive property and enters into melanocytes in the epidermis. MHY498 prevents melanogenesis in melanocytes by inhibiting the rate-limiting enzyme tyrosinase. Therefore, melanin overproduction is controlled and helps maintain normal skin brightness. In blank-SLNs group, skin brightness dropped down to below 45 over 14 days of UVB radiation, supporting the fact that blank-SLNs do not have a role in preventing melanogenesis. Ethanol and propylene glycol also have the ability to penetrate the skin.[50] They can promote MHY498 permeation from MHY solution, but cannot prevent melanogenesis effectively. The above results were confirmed by histological evaluation. In response to UV radiation, the skin produces melanin from melanocytes to neutralize the effects of radiation. Fontana–Masson staining is a common histological technique used to stain melanin black and enable melanin detection in the epidermis.[51] As illustrated in Figure 6, the melanin quantity was highest (indicated by arrow) in UV control group,

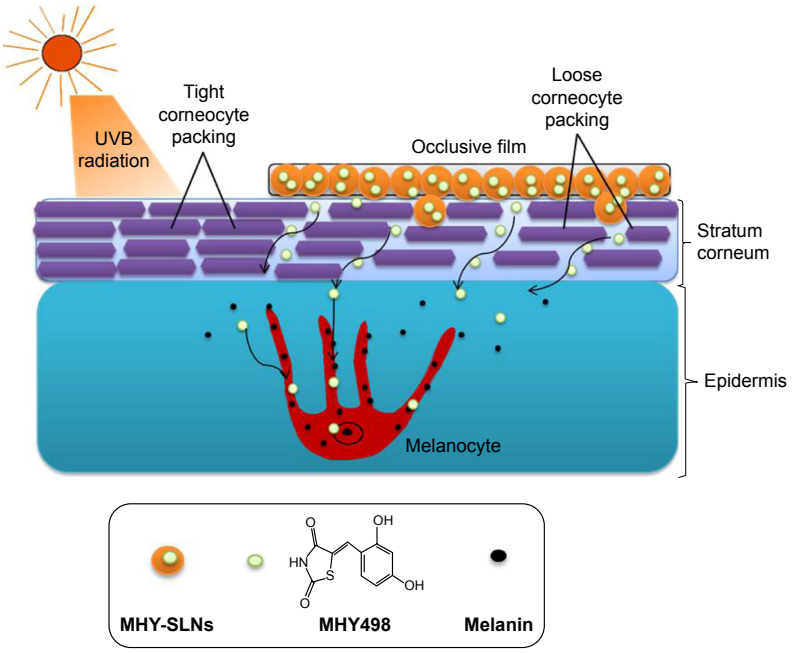

Figure 4 Proposed permeation mechanism of MHY498 from MHY-SLNs matrix through loose corneocyte packing of stratum corneum after skin application.
Abbreviations: MHY-SLNs, MHY498-loaded solid lipid nanoparticles; UVB, ultraviolet B.

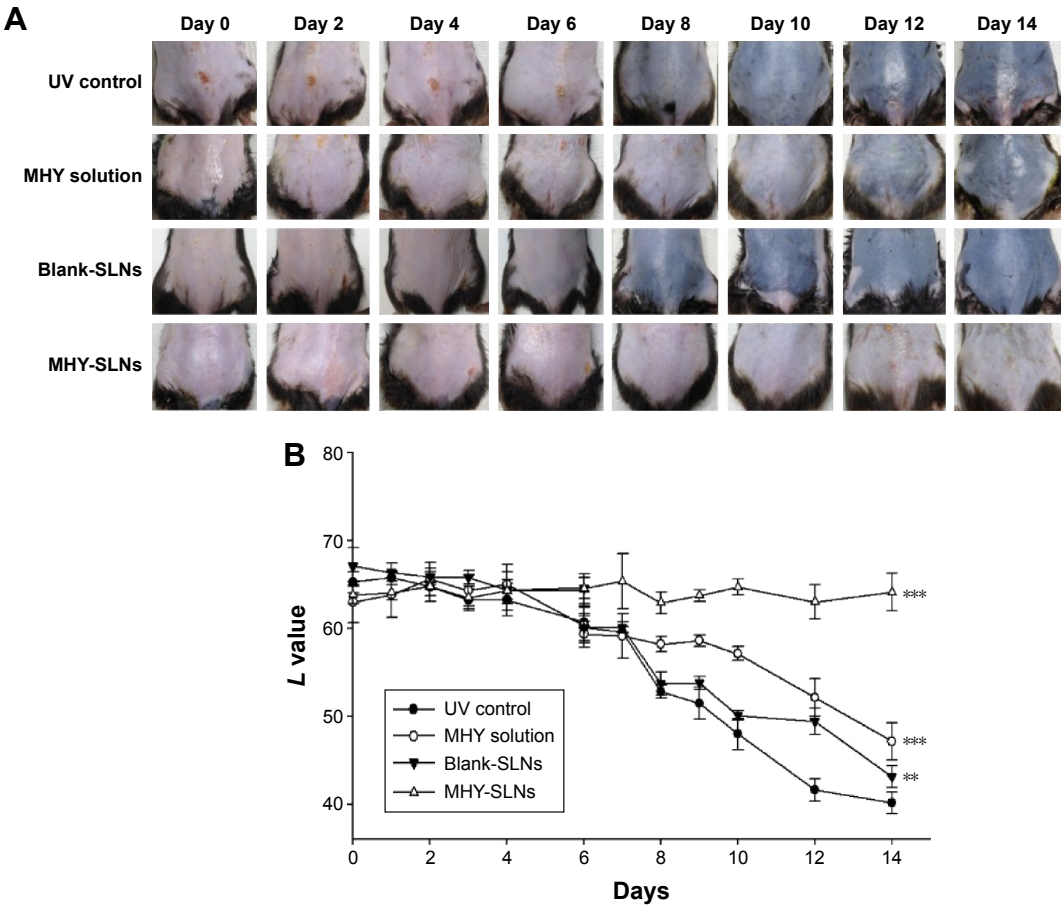

Figure 5 In vivo evaluation of MHY-SLNs.
Notes: (**A**) Qualitative skin-brightness comparison based on daily changes in skin brightness observed with the UV control, MHY solution, and MHY-SLNs groups. (**B**) Quantitative skin-brightness comparison based on reflective colorimetric measurements of skin darkening with the UV control, MHY solution, and MHY-SLNs groups. The values are presented as the mean ± SD (n=6). ***$P<0.001$ for MHY-SLNs and MHY solution group, and **$P<0.01$ for Blank-SLNs group when compared with the UV control group.
Abbreviations: MHY-SLNs, MHY498-loaded solid lipid nanoparticles; SD, standard deviation; UV control, ultraviolet control.

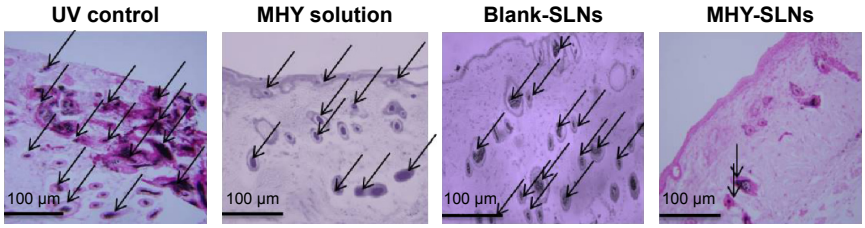

Figure 6 Fontana–Masson-stained sections of C57BL/6 skin from the UV control, MHY solution, and MHY-SLNs groups.
Notes: Black pigments indicated by the arrows signify melanin in the epidermis. All images were taken at 20× magnification.
Abbreviations: MHY-SLNs, MHY498-loaded solid lipid nanoparticles; UV control, ultraviolet control.

providing evidence of UV radiation-induced melanogenesis. In the MHY solution group, significantly greater melanin production was observed, which was indicative of ineffective melanogenesis inhibition. However, in the MHY-SLNs group, almost no melanin was found in the epidermis, which demonstrated that MHY-SLNs inhibit UVB-induced melanogenesis in an effective manner.

In vitro cytotoxicity study

The skin toxicity of topical medications is becoming a great concern.[52] The overall performance of any formulation is also related to its toxicity profile. Therefore, MHY-SLNs cytotoxicity was evaluated using the L929 mouse fibroblast cell line and compared with that of the MHY solution. The L929 cell line is commonly used in different experimental settings, such as when studying material biocompatibility and drug cytotoxicity.[53,54] As shown in Figure 7, MHY-SLNs showed no significant cytotoxicity (cell viability >90%) at concentrations of up to 400 μg MHY498/mL, whereas only 200 μg MHY498/mL was used for in vivo studies.

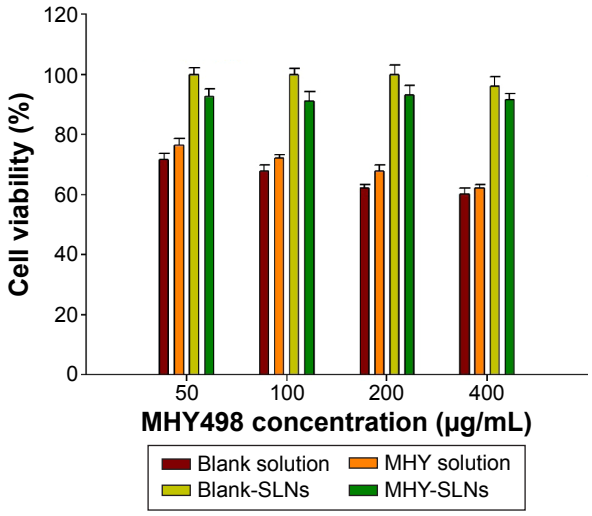

Figure 7 In vitro cytotoxicity study of MHY-SLNs and MHY solution.
Notes: The L929 mouse fibroblast cell line was used to evaluate skin cytotoxicity. The data shown represent the mean ± SD (n=4).
Abbreviations: MHY-SLNs, MHY498-loaded solid lipid nanoparticles; SD, standard deviation.

Lipids used in SLN formulation are considered nontoxic and biocompatible. Potential toxicity concerns should be considered due to the presence of stabilizers (surfactants and cosurfactants).[55,56] Poloxamer 188 and Phospholipon 90 G (used in the formulation) are nonionic compounds, which are considered the least problematic.[57] In the case of MHY solution, the cell viability was <80%, which indicated its more toxic nature. Comparing MHY solution with a blank solution indicated that toxicity might have been imparted from the solution used. It has been reported that ethanol and propylene glycol can change the lipid structures of the skin and damage the skin barrier, which might pose toxicity.[58] Moreover, the solvent concentration used was the minimum concentration required to dissolve MHY498.

Conclusion

MHY498 was successfully incorporated in SLNs with sufficient drug loading and encapsulation efficiency. MHY-SLNs were fabricated at the nanometer range and possessed occlusive properties that enhanced the skin permeation of MHY498. The results of in vitro release and in vitro skin-permeation studies revealed a prolonged release and skin permeation of MHY498 from SLN matrixes. In vivo evaluation in a C57BL/6 mouse model demonstrated that MHY-SLNs effectively prevented UVB-induced melanogenesis. MHY-SLNs were nontoxic at the minimum effective concentration. Thus, MHY-SLNs may be effective in treating hyperpigmentation.

Acknowledgment

This work was supported by a National Research Foundation of Korea (NRF) grant funded by the Korea government (MSIP; grant no 2009-0083538).

Disclosure

The authors report no conflicts of interest in this work.

References

1. Hearing VJ. Milestones in melanocytes/melanogenesis. *J Invest Dermatol*. 2011;131(E1):E1.

2. Brenner M, Hearing VJ. The protective role of melanin against UV damage in human skin. *Photochem Photobiol*. 2008;84(3):539–549.
3. Olson RL, Gaylor J, Everett MA. Skin color, melanin, and erythema. *Arch Dermatol*. 1973;108(4):541–544.
4. Halder RM, Nootheti PK. Ethnic skin disorders overview. *J Am Acad Dermatol*. 2003;48(Suppl 6):S143–S148.
5. Timilshina S, Bhuvan K, Khanal M, Marshani B, Paudyal B, Skalko-Basnet N. The influence of ethnic origin on the skin photoageing: Nepalese study. *Int J Cosmet Sci*. 2011;33(6):553–559.
6. Zonios G, Bykowski J, Kollias N. Skin melanin, hemoglobin, and light scattering properties can be quantitatively assessed in vivo using diffuse reflectance spectroscopy. *J Invest Dermatol*. 2001;117(6): 1452–1457.
7. Roméro-Graillet C, Aberdam E, Biagoli N, Massabni W, Ortonne J-P, Ballotti R. Ultraviolet B radiation acts through the nitric oxide and cGMP signal transduction pathway to stimulate melanogenesis in human melanocytes. *J Biol Chem*. 1996;271(45):28052–28056.
8. Schwahn DJ, Xu W, Herrin AB, Bales ES, Medrano EE. Tyrosine levels regulate the melanogenic response to α-melanocyte-stimulating hormone in human melanocytes: implications for pigmentation and proliferation. *Pigment Cell Res*. 2001;14(1):32–39.
9. Kameyama K, Takemura T, Hamada Y, et al. Pigment production in murine melanoma cells is regulated by tyrosinase, tyrosinase-related protein 1 (TRP1), DOPAchrome tautomerase (TRP2), and a melanogenic inhibitor. *J Invest Dermatol*. 1993;100(2):126–131.
10. Slominski A, Tobin DJ, Shibahara S, Wortsman J. Melanin pigmentation in mammalian skin and its hormonal regulation. *Physiol Rev*. 2004;84(4):1155–1228.
11. Tief K, Hahne M, Schmidt A, Beermann F. Tyrosinase, the key enzyme in melanin synthesis, is expressed in murine brain. *Eur J Biochem*. 1996; 241(1):12–16.
12. Chang TS. An updated review of tyrosinase inhibitors. *Int J Mol Sci*. 2009;10(6):2440–2475.
13. Parvez S, Kang M, Chung HS, et al. Survey and mechanism of skin depigmenting and lightening agents. *Phytother Res*. 2006;20(11):921–934.
14. Hermanns J, Pierard-Franchimont C, Pierard G. Skin colour assessment in safety testing of cosmetics. An overview. *Int J Cosmet Sci*. 2000; 22(1):67–72.
15. Kim SH, Ha YM, Moon KM, et al. Anti-melanogenic effect of (Z)-5-(2, 4-dihydroxybenzylidene)thiazolidine-2,4-dione, a novel tyrosinase inhibitor. *Arch Pharm Res*. 2013;36(10):1189–1197.
16. Ha YM, Kim JA, Park YJ, et al. Analogs of 5-(substituted benzylidene) hydantoin as inhibitors of tyrosinase and melanin formation. *Biochim Biophys Acta*. 2011;1810(6):612–619.
17. Marks R. The stratum corneum barrier: the final frontier. *J Nutr*. 2004; 134(8):2017S–2021S.
18. Morpurgo G, Catacuzzeno L, Peruzzi S, Blasi P, Fioretti B. Are tyrosinase inhibitors in sunscreens and cosmetics enhancing UV carcinogenicity? *Exp Dermatol*. 2015;24(7):546–547.
19. MuÈller RH, MaÈder K, Gohla S. Solid lipid nanoparticles (SLN) for controlled drug delivery – a review of the state of the art. *Eur J Pharm Biopharm*. 2000;50(1):161–177.
20. Müller RH, Radtke M, Wissing SA. Solid lipid nanoparticles (SLN) and nanostructured lipid carriers (NLC) in cosmetic and dermatological preparations. *Adv Drug Deliv Rev*. 2002;54(Suppl 1):S131–S155.
21. Wissing S, Kayser O, Müller R. Solid lipid nanoparticles for parenteral drug delivery. *Adv Drug Deliv Rev*. 2004;56(9):1257–1272.
22. Xu W, Lee MK. Development and evaluation of lipid nanoparticles for paclitaxel delivery: a comparison between solid lipid nanoparticles and nanostructured lipid carriers. *J Pharm Investig*. 2015;45(7):675–680.
23. Abla MJ, Singh ND, Banga AK. Role of nanotechnology in skin delivery of drugs. In: *Percutaneous Penetration Enhancers Chemical Methods in Penetration Enhancement. Verlag, Berlin, Heidelberg*: Springer; 2016:1–13.
24. Wissing S, Lippacher A, Müller R. Investigations on the occlusive properties of solid lipid nanoparticles (SLN). *J Cosmet Sci*. 2000;52(5): 313–324.
25. Ansmann A, Kawa R, Nitsche M, Gondek H, inventors; Henkel Kommanditgesellschaft Auf Aktien, assignee. Containing alkyl or alkenl oligoglycoside and fatty alcohol; cosmetics, drugs. Google Patents US 5795978 A. 1998 Aug 18.
26. So JW, Kim S, Park JS, et al. Preparation and evaluation of solid lipid nanoparticles with JSH18 for skin-whitening efficacy. *Pharma Dev Technol*. 2010;15(4):415–420.
27. Fan H, Liu G, Huang Y, Li Y, Xia Q. Development of a nanostructured lipid carrier formulation for increasing photo-stability and water solubility of phenylethyl resorcinol. *Appl Surf Sci*. 2014;288:193–200.
28. Ki DH, Jung HC, Noh YW, et al. Preformulation and formulation of newly synthesized QNT3-18 for development of a skin whitening agent. *Drug Dev Ind Pharm*. 2013;39(4):526–533.
29. Tokton N, Panichayupakaranant P. Development of ellagic acid rich pomegranate extract loaded nanostructured lipid carriers (NLC). *Int J Pharm Pharm Sci*. 2014;6:259–265.
30. Zhang H, Zhang F-M, Yan S-J. Preparation, in vitro release, and pharmacokinetics in rabbits of lyophilized injection of sorafenib solid lipid nanoparticles. *Int J Nanomedicine*. 2012;7:2901–2910.
31. Silva A, González-Mira E, García M, et al. Preparation, characterization and biocompatibility studies on risperidone-loaded solid lipid nanoparticles (SLN): high pressure homogenization versus ultrasound. *Colloids Surf B Biointerfaces*. 2011;86(1):158–165.
32. Müller R, Dingler A. The next generation after the liposomes: solid lipid nanoparticles (SLN, Lipopearls) as dermal carrier in cosmetics. *Eurocosmetics*. 1998;7(8):19–26.
33. Brewer MS, Zhu LG, Bidner B, Meisinger DJ, McKeith FK. Measuring pork color: effects of bloom time, muscle, pH and relationship to instrumental parameters. *Meat Sci*. 2001;57(2):169–176.
34. Komatsu H, Kitajima A, Okada S. Pharmaceutical characterization of commercially available intravenous fat emulsions: estimation of average particle size, size distribution and surface potential using photon correlation spectroscopy. *Chem Pharm Bull (Tokyo)*. 1995;43(8): 1412–1415.
35. Levy MY, Schutze W, Fuhrer C, Benita S. Characterization of diazepam submicron emulsion interface: role of oleic acid. *J Microencapsul*. 1994; 11(1):79–92.
36. Schwarz C, Mehnert W. Solid lipid nanoparticles (SLN) for controlled drug delivery II. Drug incorporation and physicochemical characterization. *J Microencapsul*. 1999;16(2):205–213.
37. Youshia J, Kamel AO, El Shamy A, Mansour S. Design of cationic nanostructured heterolipid matrices for ocular delivery of methazolamide. *Int J Nanomedicine*. 2012;7:2483–2496.
38. Venkateswarlu V, Manjunath K. Preparation, characterization and in vitro release kinetics of clozapine solid lipid nanoparticles. *J Control Release*. 2004;95(3):627–638.
39. Chen H, Chang X, Du D, et al. Podophyllotoxin-loaded solid lipid nanoparticles for epidermal targeting. *J Control Release*. 2006;110(2): 296–306.
40. zur Mühlen A, Schwarz C, Mehnert W. Solid lipid nanoparticles (SLN) for controlled drug delivery – drug release and release mechanism. *Eur J Pharm Biopharm*. 1998;45(2):149–155.
41. Baek J-S, Cho C-W. Comparison of solid lipid nanoparticles for encapsulating paclitaxel or docetaxel. *J Pharm Investi*. 2015;45(7): 625–631.
42. Bawa R, Audette GF, Rubinstein I. *Handbook of Clinical Nanomedicine: Nanoparticles, Imaging, Therapy, and Clinical Applications*. Vol 1. Boca Raton, FL, USA: CRC Press; 2016.
43. Williams AC, Barry BW. Penetration enhancers. *Adv Drug Deliv Rev*. 2012;64:128–137.
44. Panchagnula R, Salve PS, Thomas NS, Jain AK, Ramarao P. Transdermal delivery of naloxone: effect of water, propylene glycol, ethanol and their binary combinations on permeation through rat skin. *Int J Pharm*. 2001;219(1–2):95–105.
45. Ostrenga J, Steinmetz C, Poulsen B, Yett S. Significance of vehicle composition II: prediction of optimal vehicle composition. *J Pharm Sci*. 1971;60(8):1180–1183.

46. Chakraborty AK, Funasaka Y, Slominski A, et al. UV light and MSH receptors. *Ann N Y Acad Sci*. 1999;885(1):100–116.
47. Gilchrest BA, Park HY, Eller MS, Yaar M. Mechanisms of ultraviolet light-induced pigmentation. *Photochem Photobiol*. 1996;63(1):1–10.
48. Lin JY, Fisher DE. Melanocyte biology and skin pigmentation. *Nature*. 2007;445(7130):843–850.
49. Hoglund E, Balm P, Winberg S. Skin darkening, a potential social signal in subordinate arctic charr (*Salvelinus alpinus*): the regulatory role of brain monoamines and pro-opiomelanocortin-derived peptides. *J Exp Biol*. 2000;203(11):1711–1721.
50. Levang AK, Zhao K, Singh J. Effect of ethanol/propylene glycol on the in vitro percutaneous absorption of aspirin, biophysical changes and macroscopic barrier properties of the skin. *Int J Pharm*. 1999;181(2):255–263.
51. Prophet EB, Mills B, Arrington JB, Sobin LH. *Laboratory Methods in Histotechnology*. Washington, DC, USA: American Registry of Pathology; 1992.
52. Nohynek GJ, Antignac E, Re T, Toutain H. Safety assessment of personal care products/cosmetics and their ingredients. *Toxicol Appl Pharmacol*. 2010;243(2):239–259.
53. Nurhasni H, Cao J, Choi M, et al. Nitric oxide-releasing poly (lactic-co-glycolic acid)-polyethylenimine nanoparticles for prolonged nitric oxide release, antibacterial efficacy, and in vivo wound healing activity. *Int J Nanomedicine*. 2015;10:3065–3080.
54. Zange R, Kissel T. Comparative in vitro biocompatibility testing of polycyanoacrylates and poly (D, L-lactide-co-glycolide) using different mouse fibroblast (L929) biocompatibility test models. *Eur J Pharm Biopharm*. 1997;44(2):149–157.
55. Müller R, Maaben S, Weyhers H, Mehnert W. Phagocytic uptake and cytotoxicity of solid lipid nanoparticles (SLN) sterically stabilized with poloxamine 908 and poloxamer 407. *J Drug Target*. 1996;4(3):161–170.
56. Heydenreich AV, Westmeier R, Pedersen N, Poulsen HS, Kristensen HG. Preparation and purification of cationic solid lipid nanospheres – effects on particle size, physical stability and cell toxicity. *Int J Pharm*. 2003;254(1):83–87.
57. Weyenberg W, Filev P, Van den Plas D, et al. Cytotoxicity of submicron emulsions and solid lipid nanoparticles for dermal application. *Int J Pharm*. 2007;337(1–2):291–298.
58. Kwak S, Brief E, Langlais D, Kitson N, Lafleur M, Thewalt J. Ethanol perturbs lipid organization in models of stratum corneum membranes: an investigation combining differential scanning calorimetry, infrared and 2H NMR spectroscopy. *Biochim Biophys Acta*. 2012;1818(5):1410–1419.